

Effects of dopant concentration on structural and near-infrared luminescence of Nd³⁺-doped beta-Ga₂O₃ thin films

Cite as: Appl. Phys. Lett. **106**, 171910 (2015); <https://doi.org/10.1063/1.4919586>

Submitted: 21 January 2015 . Accepted: 21 April 2015 . Published Online: 29 April 2015

Zhenping Wu, Gongxun Bai, Qingrong Hu, Daoyou Guo, Changlong Sun, Liyuan Ji, Ming Lei, Linghong Li, Peigang Li, Jianhua Hao, and Weihua Tang



View Online



Export Citation



CrossMark

ARTICLES YOU MAY BE INTERESTED IN

[A review of Ga₂O₃ materials, processing, and devices](#)

Applied Physics Reviews **5**, 011301 (2018); <https://doi.org/10.1063/1.5006941>

[Deep ultraviolet photoconductive and near-infrared luminescence properties of Er³⁺-doped β-Ga₂O₃ thin films](#)

Applied Physics Letters **108**, 211903 (2016); <https://doi.org/10.1063/1.4952618>

[Gallium oxide \(Ga₂O₃\) metal-semiconductor field-effect transistors on single-crystal β-Ga₂O₃ \(010\) substrates](#)

Applied Physics Letters **100**, 013504 (2012); <https://doi.org/10.1063/1.3674287>

Lock-in Amplifiers
Find out more today



Zurich
Instruments

Effects of dopant concentration on structural and near-infrared luminescence of Nd³⁺-doped β -Ga₂O₃ thin films

Zhenping Wu,^{1,2} Gongxun Bai,^{3,4} Qingrong Hu,¹ Daoyou Guo,¹ Changlong Sun,¹ Liyuan Ji,⁵ Ming Lei,^{1,2} Linghong Li,⁵ Peigang Li,^{1,6} Jianhua Hao,^{3,4,a)} and Weihua Tang^{1,2,a)}

¹Laboratory of Optoelectronics Materials and Devices, School of Science, Beijing University of Posts and Telecommunications, Beijing 100876, China

²State Key Laboratory of Information Photonics and Optical Communications, Beijing University of Posts and Telecommunications, Beijing 100876, China

³Department of Applied Physics, The Hong Kong Polytechnic University, Hong Kong, China

⁴The Hong Kong Polytechnic University Shenzhen Research Institute, Shenzhen 518057, China

⁵Department of Physics, The State University of New York at Potsdam, Potsdam, New York 13676-2294, USA

⁶Center for Optoelectronics Materials and Devices, Department of Physics, Zhejiang Sci-Tech University, Hangzhou, Zhejiang 310018, China

(Received 21 January 2015; accepted 21 April 2015; published online 29 April 2015)

We have investigated structural and near-infrared (NIR) luminescence of Nd³⁺-doped β -Ga₂O₃ thin films (Nd:Ga₂O₃) with different Nd³⁺ doping concentrations. With an increase of Nd³⁺ content, the crystal lattice of the films expands, while the energy band gap shrinks. Moreover, NIR luminescence is investigated as a function of Nd³⁺ doping concentration. The measured results are related to the structural change and energy transfer of cross relaxation process ascribed to ⁴F_{3/2}—⁴I_{9/2}, ⁴F_{3/2}—⁴I_{11/2}, and ⁴F_{3/2}—⁴I_{13/2} of the phosphor films. This work implies that the enhanced NIR luminescence and blue-shift observation are associated with the lattice distortion and the variation in the crystal field of Nd: Ga₂O₃. © 2015 AIP Publishing LLC. [<http://dx.doi.org/10.1063/1.4919586>]

Lanthanide-doped semiconductors have attracted continuous attentions for their potential applications in optoelectronic devices such as optical imaging devices, waveguides, and amplifiers.^{1–7} It is well-known that the luminescence efficiency of dopant emissions could be highly improved with a wide bandgap host.⁸ Moreover, the wide bandgap semiconductors exhibit highly thermal and chemical stability, which make them ideal hosts for lanthanide ions. As one of wide bandgap semiconductors (~4.9 eV), β -Ga₂O₃ has been proved to serve as a desirable material in many fields such as solar-blind photodetector, gas sensor, electron-luminescent device, transparent conducting oxide, and field-effect transistor.^{9–12} β -Ga₂O₃ also behaves as an n-type semiconductor due to the presence of a donor band related to intrinsic oxygen deficiency.¹³ Many groups have reported the effect on the structural and luminescence properties of some lanthanide ions doped Ga₂O₃.^{14–17} Among these dopants, particular interests have been shown on neodymium (Nd) with near-infrared (NIR) emission at ~1100 nm corresponding to ⁴F_{3/2}—⁴I_{11/2} transition, which is widely used for high power laser media with a high stimulated emission cross-section.^{18,19} The related physical properties of Nd dopant have been examined in many semiconductor matrices such as TiO₂, GaN, and AlN phosphors.^{20–22} However, previous studies have seldom focused on the incorporation of Nd ion into Ga₂O₃. There are many fundamental properties of Nd:Ga₂O₃ that remain insufficiently unknown or evaluated. On the other hand, compared to powders, luminescent thin films provide several advantages, such as higher thermal stability, better adhesion to the solid surface, higher lateral

resolution from smaller grains, and reduced outgassing rate, which makes them prominent applications in flat-panel displays, light sources, and integrated optics systems.⁷ Therefore, further systematic study of the structural and luminescence properties of Nd:Ga₂O₃ film is of vital importance for the future applications. In this work, we present the results of investigating Nd doped β -Ga₂O₃ thin films with various dopant concentrations. The correlation between the optical properties and lattice distortions is studied. Spectroscopic evidence is provided for the doping of Nd ion into the β -Ga₂O₃ lattice. The crystal field analysis for the observed enhancement in NIR luminescence and blue-shift is carried out.

Nd-doped β -Ga₂O₃ films with the thickness of 200 nm were deposited on (0001) Al₂O₃ substrates with the dimension of 10 mm × 10 mm × 0.5 mm by radio frequency magnetron sputtering. A Ga₂O₃ disk embedded by several strips of Nd₂O₃ was used as the target. The Nd concentrations were controlled by solely changing the strips numbers during the deposition. The Nd concentrations in Nd: Ga₂O₃ films were determined as 0.4 mol. %, 0.8 mol. %, 1.2 mol. %, and 1.6 mol. % by the X-ray energy dispersive spectroscopy (EDS). The base pressure in the sputtering chamber was 1 × 10⁻⁴ Pa. The growth temperature and Ar gas pressure were fixed at 750 °C and 1 Pa, respectively. The power applied to the Nd:Ga₂O₃ target was set at ~80 W. The crystal structure was measured by a Bruker D8 Advance X-ray diffractometer (XRD). Ultraviolet-visible (UV-vis) absorption spectrum was taken using a Hitachi U-3900 UV-visible spectrophotometer. The valences of Nd ions were analyzed by X-ray photoelectron spectroscopy (XPS). The photoluminescence (PL) spectra were recorded using an Edinburgh FLSP920 spectrophotometer equipped with a He-Cd laser

^{a)}Authors to whom correspondence should be addressed. Electronic addresses: jh.hao@polyu.edu.hk and whtang@bupt.edu.cn

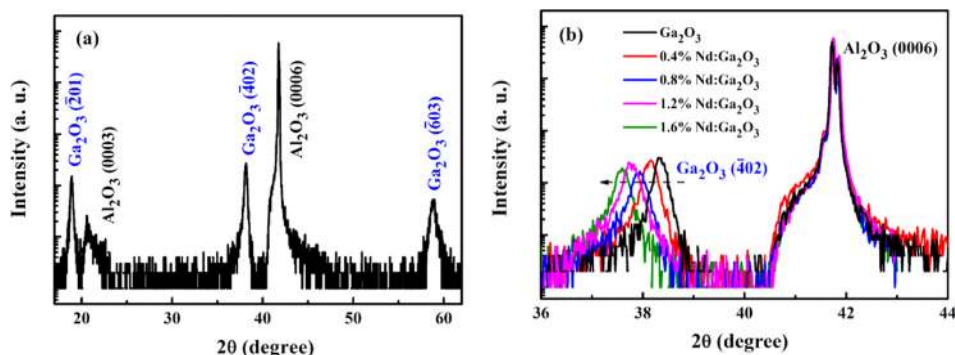


FIG. 1. (a) XRD patterns of the β -Ga₂O₃. (b) θ - 2θ spectrum in a narrow range of the Nd:Ga₂O₃ films with different doping concentration level (0%, 0.4%, 0.8%, 1.2%, and 1.6%).

(325 nm). And the laser beam with a power of 30 mW was focused on the center of the Nd:Ga₂O₃ sample. NIR PL spectra were detected with a nitrogen-cooled NIR photomultiplier tube (Hamamatsu C9940-02). All the measurements were carried out at room temperature.

The crystallinity and crystallographic orientation of the formed Nd:Ga₂O₃ films were examined by XRD. Fig. 1(a) shows the θ - 2θ spectrum of the 200 nm thick undoped β -Ga₂O₃ film deposited on (0001) sapphire single-crystal substrate. Only the ($\bar{2}01$) peak of β -Ga₂O₃ is presented along with that of the Al₂O₃ substrate. This result indicates that the β -Ga₂O₃ thin film is grown with its ($\bar{2}01$) plane normal to the Al₂O₃ substrate. Fig. 1(b) demonstrates the XRD patterns in a small angle range around the Nd:Ga₂O₃: ($\bar{4}02$) reflection peaks with various amounts of Nd-doping level (0%, 0.4%, 0.8%, 1.2%, and 1.6%). As clearly seen from the XRD patterns, the Nd doping can induce remarkable modification in the structural properties of the films. The peak position of the Nd:Ga₂O₃ ($\bar{4}02$) peaks shift to lower angles with an increase of Nd dopant concentration. It is known that monoclinic β -Ga₂O₃ lattice has two distinct crystallographic sites, where Nd ions can substitute either a highly distorted octahedral site (O_h point symmetry) or a slightly distorted tetrahedral site (T_d point symmetry). Taking into account, the magnitudes of the ionic radii (Nd³⁺: 0.983 Å, Ga³⁺ in octahedral coordination: 0.62 Å, Ga³⁺ in tetrahedral coordination: 0.47 Å), the most probable site for the Nd ions substitution is at the octahedral sites of the β -Ga₂O₃ lattice. Similar results were also drawn in Dy:Ga₂O₃, Er:Ga₂O₃, and Eu:Ga₂O₃.^{14,15,17,23} Due to the large difference of the ionic radii between the dopant ions and the Ga ions of host, the strong lattice expansion along the ($\bar{2}01$) lattice plane indicates that Nd³⁺ ions enter the Ga₂O₃ lattice substitutionally. Note that neither peaks corresponding to Nd₂O₃ nor other Nd-related phases are found in the XRD patterns, confirming that Nd³⁺ ions are well incorporated into the Ga³⁺ site. The shifts in the 2θ values corresponding to the ($\bar{2}01$) plane distance of Nd:Ga₂O₃ lattice are well reflected in the variation of the lattice distortion with the Nd³⁺ concentration. When the Nd concentration increases, the lattice distortion is gradually enhanced. The full-width at half-maximum (FWHM) of the Nd:Ga₂O₃ ($\bar{4}02$) peak was used to evaluate the dependence of crystalline quality. By employing Scherrer's formula, the average size of the crystal grains can be estimated. It is found that higher lattice distortion results in larger crystalline size, which reveals the degradation of the crystallinity of the films.

The optical absorption of the Nd:Ga₂O₃ films was characterized by UV-vis absorbance measurements to confirm the band gap energy of the samples. Fig. 2(a) shows the absorbance spectra of Nd:Ga₂O₃ film along with pure β -Ga₂O₃ film. The spectra of the host exhibit a sharp intrinsic absorption edge at the wavelength of around 250 nm, whilst those of Nd-doped samples display obvious red-shift.⁸ The band gap is fitted by extrapolating the linear region of the plot $(\alpha h\nu)^2$ versus $h\nu$, as shown in the inset of Fig. 2(a). The bandgap decreases from 4.93 eV for pure β -Ga₂O₃ to 4.61 eV for 1.6% Nd:Ga₂O₃ film. Such reduction of the band gap could be attributed to new unoccupied electron states in the gap below the conduction band edge due to the location of Nd ions on the substitutional sites of Ga₂O₃. In fact, the observed red-shift in the band gap was found to correlate with the lattice distortions reflected in the d spacing of ($\bar{2}01$) plane well, as shown in Fig. 2(b). A larger d spacing is expected to result in a narrow band gap, which is similar to the band gap variation reported by other groups.^{20,24,25}

The deposited Nd:Ga₂O₃ (1.2%) films were characterized using XPS to illustrate the chemical compositions and chemical states of oxide films.^{26,27} The charge-shift spectrum was calibrated using the fortuitous C 1s peak at 284.8 eV. It is noted that two symmetrical peaks of Ga 2p_{1/2} and Ga 2p_{3/2} were located at 1145.5 eV and 1118.5 eV, respectively (Fig. 3(a)). The separation distance between these two peaks is about 27 eV, which is in good agreement with the binding energy of the Ga 2p ($\Delta = 26.8$ eV).²⁸ Fig. 3(b) reveals the high resolution XPS spectra of Nd 3d₃ and Nd 3d₅ peaks, centered at 1005.7 eV and 982.9 eV, respectively. Our measured values are slightly smaller than the standard data for Nd 3d₃ and Nd 3d₅, suggesting a potential host effect from Ga₂O₃ on the chemical environment of Nd. Therefore, XPS results confirmed that Nd atoms have been effectively incorporated into the oxide matrix and participate in the chemical bonding. The O 1s peak is split into two peaks, as shown in Fig. 3(c). The main peak at 530.8 eV could be assigned to the oxygen in Ga₂O₃ lattice, while the peak at 532.1 eV could be due to the C/O bonds related to carbonaceous contamination.²⁹ The compositional ratio of Ga-to-O is about 1:1.43, which is close to the stoichiometric ratio (Ga₂O₃: Ga-to-O = 1:1.5), indicating the presence of oxygen vacancies in the films.

Fig. 4(a) shows the NIR PL spectra of Nd:Ga₂O₃ thin films with different doping concentrations measured at room temperature. Compared to undoped β -Ga₂O₃ film, the pronounced NIR PL emission consists of three bands, corresponding to the infra-4f transitions of Nd³⁺ ions from ⁴F_{3/2} level to

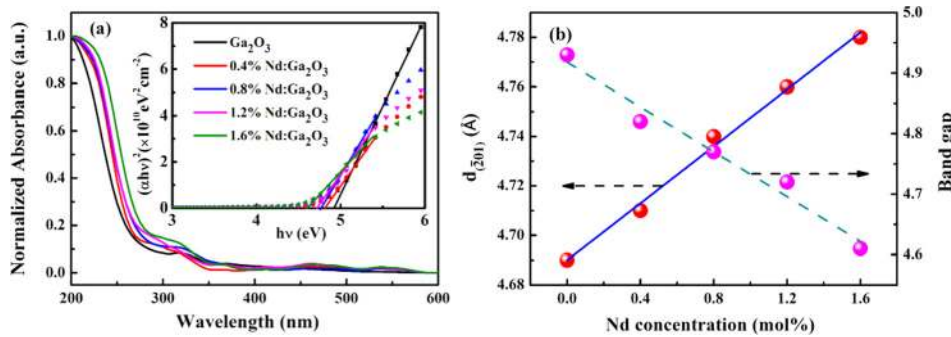


FIG. 2. (a) Absorption spectra of Nd:Ga₂O₃ thin films compared with that of undoped β -Ga₂O₃ thin film and the plot of $(xh\nu)^2$ versus $h\nu$ in the inset. (b) Nd doping concentration dependence of (201) lattice plane distance and the band gap, respectively.

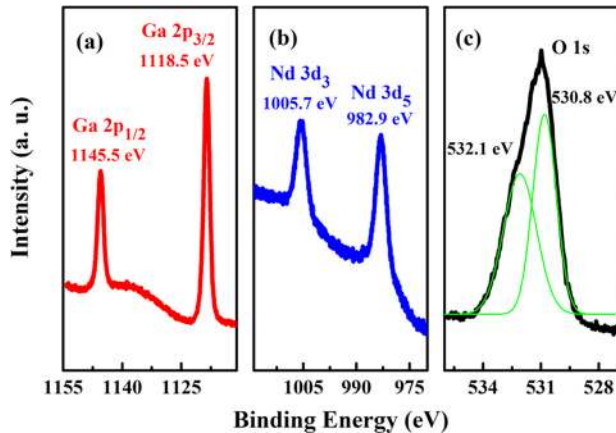


FIG. 3. XPS spectra of Ga 2p (a), Nd 3d (b), and O 1s (c) core level for Nd:Ga₂O₃ (1.2%) thin film.

$^4I_{9/2}$ (~ 905 nm), $^4I_{11/2}$ (~ 1067 nm), and $^4I_{13/2}$ (~ 1339 nm) levels, respectively. As seen, the emission intensity can be remarkably enhanced with increasing Nd³⁺ doping concentration in the Nd:Ga₂O₃ films. An enhancement factor of main $^4F_{3/2}$ – $^4I_{11/2}$ transition band can reach up to 2.3. As discussed above, the distorted octahedral site with an inversion center should be more suitable to accommodate Nd ions, presenting the selection rules forbidding all 4f–4f electric dipole (ED) transitions. With Nd dopant concentration increases, the c-axis of the lattice elongates (Fig. 2(b)) and promotes the structure asymmetry of the Ga₂O₃ host, approaching lower symmetry around Nd³⁺ ions. In principle, the lower symmetry on the site of Nd ions means that the more uneven crystal-field

components can mix opposite-parity into 4f configurational levels and subsequently increase the ED transition probabilities of the dopant ions. Herein, the increase in the ED transition probabilities relating to the elongation of d spacing of (201) plane should be responsible for the enhancement of NIR PL emission. Note that no corresponding excitation peaks related to Nd³⁺ ions were seen in the UV-Vis absorption spectra. Thus, the direct UV excitation of Nd³⁺ ions in Nd:Ga₂O₃ can be negligible.^{19,20} The above-mentioned results demonstrate the existence of efficient energy transfer (ET) from the electron-hole pairs created in the Ga₂O₃ host to Nd³⁺ ions. In this process, the Ga₂O₃ will act as an effective light harvest to absorb UV photons and subsequently transfer energy to Nd³⁺ ions and thereby resulting in the typical luminescence of the Nd³⁺ ions. Similar observations have been reported in Nd:SrTiO₃, Nd:TiO₂, etc.^{19,30} In our study, the excitation energy of incident light is lower than the band gap of Nd:Ga₂O₃. Owing to the existence of oxygen vacancy defects in the films, hence, the ET process between the Ga₂O₃ host and Nd ion might be as follows. Through ground state absorption (GSA) process, the electrons are excited from the valence band to the donor band (oxygen vacancy) by the light source. The released energy due to the recombination of electrons in the defect state with the photogenerated holes can transfer to the excited states of the Nd ions; thereby, NIR emissions of Nd take place. Notably, the NIR emission bands from Nd:Ga₂O₃ thin films present an obvious blue-shift, the main luminescent peak ($^4F_{3/2}$ – $^4I_{11/2}$) shifts from 1077 nm to 1065 nm (inset of Fig. 4(a)). The observed phenomena can be explained by the variation in the crystal field around Nd³⁺ ions, caused by

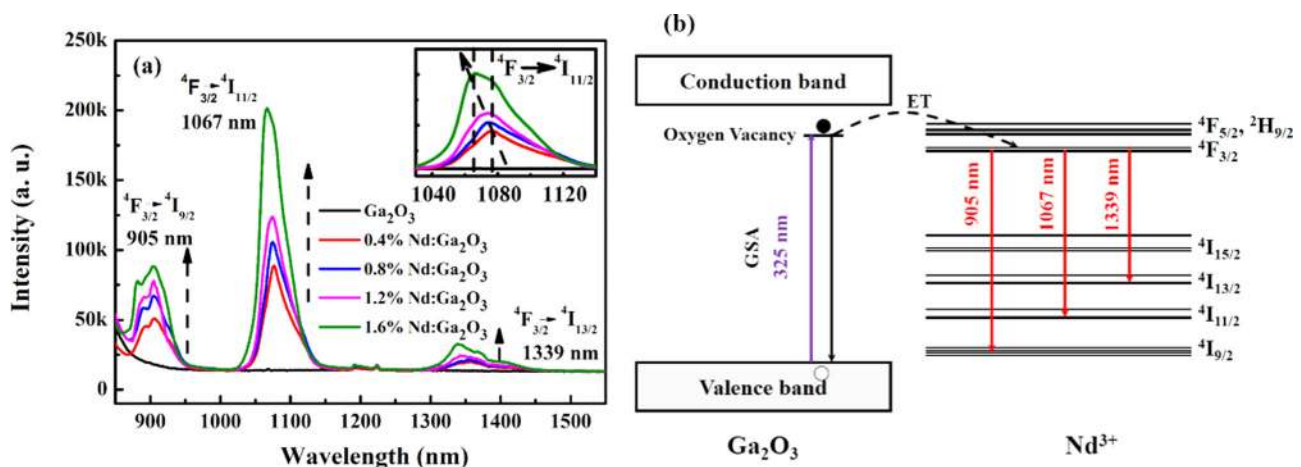


FIG. 4. (a) NIR PL spectra of Nd:Ga₂O₃ films with different doping concentrations. Inset shows the enlarged PL spectra around 1080 nm. (b) Energy level diagram of Ga₂O₃ and Nd³⁺, as well as the proposed mechanisms less than 325 nm laser excitation.

lattice distortion. As discussed above, with increasing the Nd concentration, the lattice distortion is gradually enhanced. The increase of the octahedral distortion leads to the enhancement in the Stark splitting of the $^4F_{3/2}$ multiplet. Thus, the enhanced Stark emitting levels are splitted from the $^4F_{3/2}$ state, causing the blue-shift.³¹

In conclusion, monoclinic Nd:Ga₂O₃ thin films with a preferable ($\bar{2}01$) orientation were grown on α -Al₂O₃ (0001) substrates by radio frequency magnetron sputtering. The structural and optical spectroscopy of Nd:Ga₂O₃ thin films have been systematically investigated. The evolution of lattice expansion and optical spectra with increasing the doping concentration shows the chemical substitution of Nd³⁺ ions into the Ga₂O₃ crystal lattice. The lattice distortion and the variation in the crystal field play important roles in the observed peak intensity enhancement and wavelength blue-shifts of NIR luminescence. These results may provide a new insight for further various optoelectronics applications from Nd:Ga₂O₃ films.

This work was supported by the National Natural Science Foundation of China (Nos. 61274017, 51172208, 11404029, and 51272218), Beijing Natural Science Foundation (No. 2154055), Fund of State Key Laboratory of Information Photonics and Optical Communications (BUPT), the Fundamental Research Funds for the Central Universities (Grant No. 2014RC0906), and China Postdoctoral Science Foundation Funded Project (Grant No. 2014M550661).

¹S. C. Erwin, L. J. Zu, M. I. Haftel, A. L. Efros, T. A. Kennedy, and D. J. Norris, *Nature* **436**, 91–94 (2005).

²X. Teng, Y. H. Zhu, W. Wei, S. C. Wang, J. F. Huang, R. Naccache, W. B. Hu, A. I. Y. Tok, Y. Han, Q. C. Zhang, Q. L. Fan, W. Huang, J. A. Capobianco, and L. Huang, *J. Am. Chem. Soc.* **134**, 8340–8343 (2012).

³D. T. Tu, L. Q. Liu, Q. Ju, H. M. Zhu, R. F. Li, and X. Y. Chen, *Angew. Chem. Int. Ed.* **50**, 6306–6310 (2011).

⁴G. X. Bai, M. K. Tsang, and J. H. Hao, *Adv. Opt. Mater.* **3**, 416 (2015).

⁵Z. P. Wu, Y. Zhang, G. X. Bai, W. H. Tang, J. Gao, and J. H. Hao, *Opt. Express* **22**, 29014–29019 (2014).

⁶F. Wang and X. G. Liu, *J. Am. Chem. Soc.* **130**, 5642–5643 (2008).

⁷Y. Zhang and J. H. Hao, *J. Mater. Chem. C* **1**, 5607–5618 (2013).

⁸P. N. Favennec, H. Lharidon, M. Salvi, D. Moutonnet, and Y. Leguillou, *Electron. Lett.* **25**, 718–719 (1989).

⁹D. Y. Guo, Z. P. Wu, P. G. Li, Y. H. An, H. Liu, X. C. Guo, H. Yan, G. F. Wang, C. L. Sun, L. H. Li, and W. H. Tang, *Opt. Mater. Express* **4**, 1067–1076 (2014).

¹⁰P. Wellenius, A. Suresh, and J. F. Muth, *Appl. Phys. Lett.* **92**, 021111 (2008).

¹¹D. Y. Guo, Z. P. Wu, Y. H. An, X. C. Guo, X. L. Chu, C. L. Sun, L. H. Li, P. G. Li, and W. H. Tang, *Appl. Phys. Lett.* **105**, 023507 (2014).

¹²C. H. Hsieh, M. T. Chang, Y. J. Chien, L. J. Chou, L. J. Chen, and C. D. Chen, *Nano Lett.* **8**, 3288–3292 (2008).

¹³J. B. Varley, J. R. Weber, A. Janotti, and C. G. Van de Walle, *Appl. Phys. Lett.* **97**, 142106 (2010).

¹⁴H. M. Zhu, R. F. Li, W. Q. Luo, and X. Y. Chen, *Phys. Chem. Chem. Phys.* **13**, 4411–4419 (2011).

¹⁵G. G. Li, C. Peng, C. X. Li, P. A. P. Yang, Z. Y. Hou, Y. Fan, Z. Y. Cheng, and J. Lin, *Inorg. Chem.* **49**, 1449–1457 (2010).

¹⁶J. H. Hao, Z. D. Lou, I. Renaud, and M. Cocivera, *Thin Solid Films* **467**, 182–185 (2004).

¹⁷Y. Tokida and S. Adachi, *Jpn. J. Appl. Phys., Part 1* **52**, 101102 (2013).

¹⁸D. Breard, F. Gourbilleau, A. Belarouci, C. Dufour, and R. Ria, *J. Lumin.* **121**, 209–212 (2006).

¹⁹Y. Yang, C. Y. Lv, C. Zhu, S. Li, X. Y. Ma, and D. R. Yang, *Appl. Phys. Lett.* **104**, 201109 (2014).

²⁰R. Pandiyan, V. Micheli, D. Ristic, R. Bartali, G. Pepponi, M. Barozzi, G. Gottardi, M. Ferrari, and N. Laidani, *J. Mater. Chem.* **22**, 22424–22432 (2012).

²¹G. D. Metcalfe, E. D. Readinger, H. E. Shen, N. T. Woodward, V. Dierolf, and M. Wraback, *Phys. Status Solidi C* **6**, S671–S674 (2009).

²²G. D. Metcalfe, E. D. Readinger, R. Enck, H. G. Shen, M. Wraback, N. T. Woodward, J. Poplawsky, and V. Dierolf, *Opt. Mater. Express* **1**, 78–84 (2011).

²³T. Biljan, A. Gajovic, and Z. Meic, *J. Lumin.* **128**, 377–382 (2008).

²⁴K. Kaneko, T. Nomura, I. Kakeya, and S. Fujita, *Appl. Phys. Express* **2**, 075501 (2009).

²⁵W. Mi, X. J. Du, C. N. Luan, H. D. Xiao, and J. Ma, *RSC Adv.* **4**, 30579 (2014).

²⁶Z. B. Yang, W. Huang, and J. H. Hao, *Appl. Phys. Lett.* **103**, 031919 (2013).

²⁷J. H. Hao, J. Gao, Z. Wang, and D. P. Yu, *Appl. Phys. Lett.* **87**, 131908 (2005).

²⁸D. Y. Guo, Z. P. Wu, Y. H. An, X. L. Chu, C. L. Sun, M. Lei, L. H. Li, L. X. Cao, P. G. Li, and W. H. Tang, *J. Mater. Chem. C* **3**, 1830 (2015).

²⁹H. Y. Xu, Y. C. Liu, C. S. Xu, Y. X. Liu, C. L. Shao, and R. Mu, *Appl. Phys. Lett.* **88**, 242502 (2006).

³⁰T. Fix, H. Rinnert, M. G. Blamire, A. Slaoui, and J. L. MacManus-Driscoll, *Sol. Energy Mater. Sol. Cells* **102**, 71–74 (2012).

³¹U. R. Rodriguez-Mendoza, S. F. Leon-Luis, J. E. Munoz-Santiuste, D. Jaque, and V. Lavin, *J. Appl. Phys.* **113**, 213517 (2013).